In presenting this thesis in partial fulfillment of the requirements for an advanced degree at Idaho State University, I agree that the Library shall make it freely available for inspection. I further state that permission to download and/or print my thesis for scholarly purposes may be granted by the Dean of the Graduate School, Dean of my academic division, or by the University Librarian. It is understood that any copying or publication of this thesis for financial gain shall not be allowed without my written permission.

Signature _____

Date _____

Investigation of Tritium Gaseous Effluent Release Interception by Snow Precipitation at Cook Nuclear Power Plant

by
Kent Fisher

A thesis
submitted in partial fulfillment
of the requirements for the degree of
Master of Science in the Department of Nuclear Engineering and Health Physics
College of Science and Engineering
Idaho State University
August 2016

To the Graduate Faculty:

The members of the committee appointed to examine the thesis of Kent Fisher find it satisfactory and recommend that it be accepted.

_____

Richard Brey,
Major Advisor

_____

Thomas Gesell,
Committee Member

_____

Dewayne Derryberry,
Graduate Faculty Representative

Acknowledgements

The contributions of the Environmental Department at Cook Nuclear Power Plant cannot be overlooked in the conduct of this study. Without the assistance received at the facility from providing data to sampling snow, this project would not have been possible.

Special thanks to Dr. Harris for molding and guiding this project. The many times I was lost and frustrated you kept it on track and moving forward.

My undying gratitude goes to Dr. Derryberry. Without your guidance in statistics and analysis I would not have been able to see even half of the results and conclusions presented in this paper. You opened the black box that is statistics and illuminated it just a little bit more.

Further thanks to Dr. Miller for allowing me to hitch my wagon to this project you've been working for many years.

And certainly not least, I owe Dr. Brey my eternal gratitude for you guidance, skillful editing, and for patiently allowing me to continue this project.

I wish to thank my family for putting up with the late nights and long weekends spent analyzing data and writing this paper. Without your patience and love I could not have finished this project.

Table of Contents

List of Figures…… vi
List of Tables……vii
Abstract……viii
1. Introduction…… 1
1.1 Nuclear Power Reactors…… 1
1.2 Tritium…… 4
1.3 Background…… 7
2. Literature Review…….. 10
3. Methods and Materials……...13
3.1 Determination of Tritium Interception Rate……..... 13
3.2 Determination of Correlation Between Data…… 18
4. Results and Discussion…….. 23
4.1 Determination of Tritium Interception Rate……..... 23
4.2 Determination of Correlation Between Data…… 26
5. Conclusions……27
5.1 Determination of Tritium Interception Rate……..... 27
5.2 Determination of Correlation Between Data…… 27
5.3 Future Research……..... 28
Appendix A Data Tables…….. A1

List of Figures

Figure 1: Illustration of a pressurized water reactor (USNRC, 2016)…… 3
Figure 2: Illustration of a boiling water reactor (USNRC, 2016)……4
Figure 3: General wind corridors at Cook Nuclear Power Plant …….. 15
Figure 4: Typical Gaussian Plume centerline determination……16
Figure 5: Cook Nuclear Power Plant SFP and Units 1 & 2 tritium concentrations over time……..... 19
Figure 6: Snow sample data graphed against tritium release data ……..... 20
Figure 7: Spent fuel pool concentration data graphed against tritium release data……... 20
Figure 8: Unit 1 concentration data graphed against tritium release data …… 21
Figure 9: Unit 2 concentration data plotted against tritium release data …….…..…… 21
Figure 10: All tritium interception rate observations…….……24
Figure 11: Frequency plot of interception rate observations…….…… 25

List of Tables

Table 1: Comparative Chart of all Three Data Sets……..A1
Table 2: Tritium interception rate calculation results……...A2
Table 3. Regression analysis results before imputed values……A3
Table 4. Regression analysis results after imputed values……A3

Abstract

The purpose of this study was to determine the rate at which snow precipitation intercepts tritium from air and determine if any correlation exists between the tritium concentrations of the spent fuel pool, the primary cooling loops of both pressurized water reactor units onsite, the gaseous releases of tritium, tritium concentrations in snow samples. The rate at which snow precipitation intercepts gaseous tritium released by Cook Nuclear Power Plant likely falls within the range between $1x10^{-5}$ s^{-1} and $1x10^{-7}$ s^{-1} for the conditions at the site. This reflects averages of data accumulated over long periods of time that were created by varying environmental conditions during the sampling period. Analysis of the data showed no correlation between tritium concentrations of either of the individual unit cooling systems and the tritium releases. Moreover, no correlation between the spent fuel pool tritium concentrations and the tritium releases was observed and no correlation was established between the gaseous tritium releases and the snow concentrations of tritium. The poor time resolution of the data available was a significant factor in the results of this study.

1. Introduction

1.1 Nuclear Power Reactors

The United States currently has 99 operating commercial nuclear power plants spread across 30 states providing 19.5% of the nation's electricity (NEI 2015). These power reactors are all light-water reactors (LWR) and are divided into two categories: 65-pressurized water reactors (PWR) and 34-boiling water reactors (BWR) (NEI 2015).

Natural uranium consists of 0.7% ^{235}U and 99.3% ^{238}U (Baum et al 2002, Lederer et al 1978). Civilian nuclear power reactors use uranium oxide (UO_2) that is about 3% enriched ^{235}U (Eisenbud and Gesell 1997). Uranium oxide is fabricated into pellets which are encased in a cladding to prevent fission products from being released from the fuel into the coolant (Eisenbud and Gesell 1997). The encased pellets further encased in tubes that are referred to as a fuel rod. The fuel rods are arranged into bundles which are subsequently arranged within the core of the nuclear reactor according to whatever grid pattern is prescribed for the particular reactor (Eisenbud and Gesell 1997).

The fuel is consumed by a fission reaction in the core of the nuclear reactor which involves the absorption of a neutron into the nucleus of a ^{235}U, ^{239}Pu, or ^{238}U atom leading to splitting the nucleus into two product fragments, and the release of two or three neutrons, thus growing and multiplying the neutron population (Eisenbud and Gesell 1997, Tsoulfanidis and Landsberger 2011, Ahmed 2007, Turner 1995, Martin 2013, Cember and Johnson 2009). Uranium-235 is used as the primary initial fuel within commercial nuclear power plants (LWRs) within the United States of America. The excess ^{238}U present eventually leads to the creation of ^{239}Pu. The Canadians depend on a

slightly different approach in their heavy water reactors (HWRs) or Canadian Deuterium-Uranium (CANDU) reactors (Jacobs 1968, Eisenbud and Gesell 1997, World Nuclear Association 2016). Since heavy water has a lower thermal neutron cross section it is feasible to maintain a chain reaction with the minor 0.7% ^{235}U available in natural uranium. But similar to light water reactors, these systems also take advantage of the neutron bombardment of ^{238}U leading to the creation of ^{239}Pu (World Nuclear Association 2016). Fission of the uranium fuel, initially predominantly ^{235}U in the case of the power plant in this study, is accompanied by the release of 190 to 200 MeV of energy, which is ultimately dissipated as heat (Cember and Johnson 2009). Heat for generating steam to drive a turbine is the purpose of the entire design. The heat is removed from the core by the coolant, which in the LWR is natural water. The coolant is converted to steam, drives the steam turbines, and produces electricity. The exact manner in which the coolant is converted to steam and circulates between the core and the steam turbines is determined by the specific design; that is, whether the power plant is a PWR or BWR design. This paper will focus on the PWR design of Cook Nuclear Power Plant.

The PWR (see Figure 1) is designed with a central core (where the fission reaction occurs), a primary coolant loop (which circulates between the reactor core and the heat exchanger), and the secondary coolant loop (which circulates between the heat exchangers and the steam turbines) (Eisenbud and Gesell 1997, The Virtual Nuclear Tourist 2005). The PWR maintains highly pressurized coolant at more than 2,000 psi (Eisenbud and Gesell 1997). This high pressure allows the coolant to transfer the heat but prevents the water from boiling (Eisenbud and Gesell 1997, The Virtual Nuclear Tourist 2005). The primary coolant loop transfers the heat to the secondary coolant loop

through a heat exchanger (Eisenbud and Gesell 1997). The heat exchanger is used to prevent mixing of coolant and in theory; this isolates radioactive material to the primary coolant loop (Eisenbud and Gesell 1997). The coolant in the secondary loop boils and produces the steam which drives the steam turbines (Eisenbud and Gesell 1997, The Virtual Nuclear Tourist 2005). Leakage of water and radioactive materials between the primary coolant loop and the secondary coolant loop is possible, but counter to the intended design (Eisenbud and Gesell 1997). The BWR (see Figure 2) does not use multiple loops with a heat exchanger (Eisenbud and Gesell 1997). In a BWR the water is allowed to boil directly in the core and circulate to the steam turbines (Eisenbud and Gesell 1997).

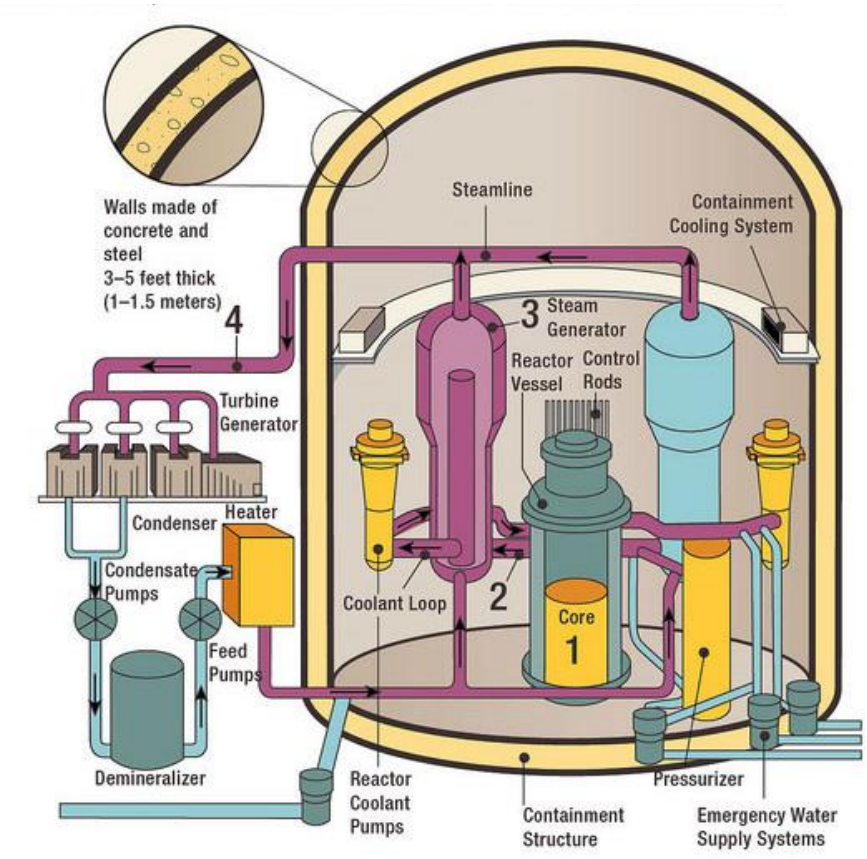

Figure 1. Illustration of a pressurized water reactor (USNRC, 2016)

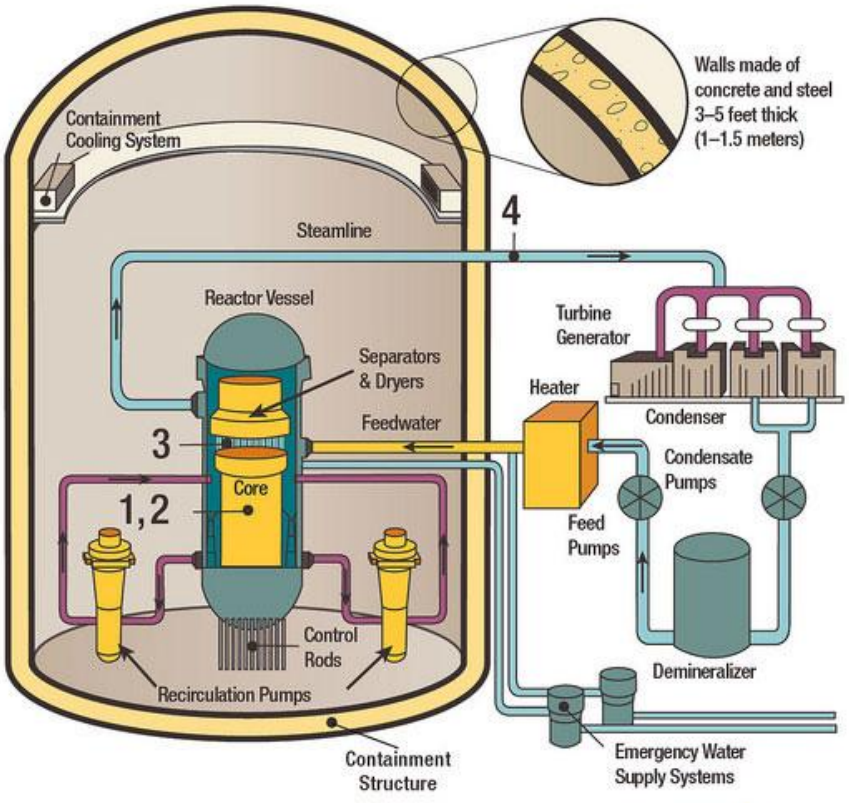

Figure 2. Illustration of a boiling water reactor (USNRC, 2016)

1.2 Tritium

Hydrogen has three isotopes. Elemental hydrogen is represented by the symbol ^{1}H or H and possesses a single proton nucleus with a single orbital electron. Deuterium is represented by the symbol ^{2}H or D and possesses a single proton and single neutron nucleus with a single orbital electron. Tritium is represented by the symbol ^{3}H or T and possesses a single proton and double neutron nucleus with a single orbital electron. Elementally hydrogen is found as a diatomic gas, H_2. In the gas phase, HT is the dominant chemical form of tritium in the stratosphere but HTO is the dominant chemical form of tritium in the troposphere (Jacobs 1968, Chi et al 2003). T_2O and T_2 are extremely rare because the concentration of environmental elemental hydrogen is much

greater than environmental tritium and thus the statistical opportunity for the formation of these compounds is simply too low for them to be prevalent in appreciable quantities (Jacobs 1968, Chi et al 2003). Once tritium, usually in the chemical form HTO, is taken into a biological organism it can be incorporated into the tissue of the organism and may become known as organically bound tritium (OBT). Tritium decays slowly to helium, at a half-life of 12.28 y, and only emits one negatron beta particle with a maximum energy of 18.6 keV and an average energy of 5.7 keV (Shleien 1992, Jacobs 1968, Chi et al 2003). Tritium, then, is not an external hazard to humans since the beta particle it emits cannot penetrate the outer layer of dead skin; however tritiated water (HTO) can enter the body both by inhalation and skin absorption (Harris et al 2008, Jacobs 1968).

Tritium is produced in a nuclear reactor by four primary processes: fission, neutron irradiation of lithium, neutron irradiation of boron, and neutron irradiation of deuterium (Jacobs 1968, Luykx and Fraser 1986). As previously discussed, the process of fission splits the uranium atom into by-product atoms. Tritium is one possible by-product of fission at an incidence of $1x10^{-4}$ to $2x10^{-4}$ atoms per fission (Jacobs 1968). Tritium is produced by the neutron bombardment of ^{10}B in the control rods or the coolant by thermal neutrons. PWRs use control rods constructed with boron to remove neutrons from the core and shape the neutron field (Monterrosa et al 2012). Boron is also added to the coolant as a neutron absorber or chemical shim thus allowing for more highly enriched fuel at the beginning of core life (Monterrosa et al 2012). Tritium is also produced in the coolant by the bombardment of ^{6}Li by thermal neutrons and ^{7}Li by fast neutrons (Jacobs 1968). Lithium fluoride is added to the PWR coolant for two reasons according to the World Nuclear Association (2014). First it is used to stabilize the water

chemistry and second to prevent corrosion that can be caused by the boric acid additive previously discussed.

As briefly discussed, the coolant in an HWR is predominantly HDO in which one hydrogen atom of water is replaced by deuterium. During neutron bombardment of the coolant HDO is transmuted to HTO and the production of tritium by this process is as significant as the production of tritium by fission; except fission-produced tritium is usually trapped in the fuel by the cladding (Jacobs 1968, Luykx and Fraser 1986, Chi et al 2003). The concentration of deuterium in a LWR is the same as that in natural water, so neutron activation does not play a significant role in the production of tritium (Jacobs 1968). Fission is the most significant source of tritium production in an LWR, and when the fuel elements are encased in stainless steel cladding, the concentration of HTO in the coolant is about 100 times higher than when the fuel is clad with Zircaloy (Jacobs 1968, Luykx and Fraser 1986). However, tritium production from ^{10}B irradiation by neutrons is the greatest producer of tritium in PWR coolant (Monterrosa et al 2012).

The production of tritium in nuclear reactors leads to a buildup of tritium concentration in the coolant and spent fuel pools (Jacobs 1968, Harris et al 2008, Hinchcliffe 2010). Tritium produced in the fuel by fission sometimes diffuses through the cladding into the coolant (Jacobs 1968). The diffusion rate of tritium through the cladding depends very greatly on the construction material of the cladding and cladding integrity (Jacobs 1968, Luykx and Fraser 1986). As previously stated, stainless steel allows tritium to diffuse into the coolant with more ease than the Zircaloy cladding (Jacobs 1968, Luykx and Fraser 1986). During the refueling process, old fuel elements are moved to the spent fuel pool within a reactor complex. Tritium diffuses from the old

fuel elements into the spent fuel pool in the same manner it does within the coolant of the reactor core. Over time, because of its long half-life, the concentration of tritium within the spent fuel pool gradually rises (Harris et al 2008, Hinchcliffe 2010).

Nuclear reactor coolant cannot indefinitely sustain the buildup of contaminants and fission products while simultaneously sustaining normal operation. Normal filtering and processing systems are in place to remove contaminants from the coolant in order to allow continued and efficient operation (Hinchcliffe 2010). Some products of this processing are released as gaseous effluents, liquid effluents, or held in waste tanks for decay and storage. Tritium, specifically, can be released, depending on the conditions of the facility license, as liquid or gaseous effluents. Releases of radioactive effluents are carefully monitored, recorded, and reported.

1.3 Background

The Cook Nuclear Power Plant is a two-unit PWR facility situated on 650 acres adjacent to Lake Michigan (Hinchcliffe 2010). Unit 1 began commercial operation in 1975 and Unit 2 began commercial operation in 1978 (Harris et al 2008). Gaseous effluents, including HTO, are released from monitored vents atop each of the respective containment buildings at a height of 45 meters (Harris et al 2008). During 2007, release of tritium became an issue of concern for operations of the Cook Nuclear Power Plant in Bridgeman, Michigan when tritium was detected in samples of water from the facility's north storm drain outfall (Hinchcliffe 2010, Harris et al 2008).

The result of the investigation into the source of tritium in the north storm drain outfall at the Cook Nuclear Power Plant revealed two sources: primarily air conditioning

condensate (recapturing tritium from the gaseous effluent releases) and interception of the tritium gaseous effluent releases by rain precipitation draining to the outfall (Harris et al 2008). A slight relationship between the rising concentration of tritium over time in the spent fuel pool and the rising concentrations of gaseous releases over time was established by Hinchcliffe (2010).

Hinchcliffe (2010) primarily studied tritium washout by rain and only briefly touched on tritium washout by snow. Hinchcliffe had some trouble with the snow data which rendered it mostly useless for calculating washout coefficients. The data set available to Hinchcliffe included some "fresh snow" collections, that is snow collected in a snow gauge during a snow precipitation event, and "old snow" collections, that is snow cores and collections done from snow drifts and snow packs. Hinchcliffe stated in his thesis that the "old snow" collections were subjected to mixing caused by plowing and blowing wind and, therefore, were questionable data since the integrity of the samples had been disturbed.

The tritium interception rate is the number of HTO molecules per second intercepted by precipitation as it is falling to the ground. The HTO is released from a stack and disperses into the atmosphere as a plume. As precipitation falls, it passes through the plume on the way to the ground. The amount of time the precipitation takes to pass through the plume directly affects how much HTO it will intercept and absorb. As the HTO is taken up by the precipitation, it is removed from the plume and carried to the ground. In the case of snow, it is possible for the tritium to be held in the snow all winter and released in the spring with the thaw. The interception rate allows for estimation of the amount of tritium released from a facility which has the potential to be

intercepted by precipitation and contribute to public doses in ways not previously taken into account.

The equation, from Davis (1997), used to calculate the tritium interception rate is a variant of the Gaussian Plume model. It is important in light of the meteorological conditions of the Cook Nuclear Power Plant complex to understand the limitations of the Gaussian Plume model for calculating dispersion of airborne particles and gases. The model assumes the release rate of whatever is being measured, in this case tritium, is constant (Harris 2015, Allen, Durrenberger 2015). The model assumes all meteorological factors are continuous over the measurement period and applies strictly to straight-line plumes (Harris 2015, Allen, Durrenberger 2015). The model cannot account for extreme turbulence, building wake, and situations in which wind shear or some other forces change the direction of the plume (Harris 2015, Allen, Durrenberger 2015). The model also assumes the dispersion of the contaminant is Gaussian about the centerline in the vertical and horizontal planes.

2. Literature Review

Gaseous tritium interception by rain has been well studied. Tritium interception by snow has not been treated in the literature with such detail. Several articles treating tritium interception by snow will be reviewed here, but all are after-the-fact reviews of old data collected incident to other purposes. Three papers are of interest to a discussion of tritium interception by snow precipitation.

The first to be published was Papadopoulos et al (1986). Papadopoulos et al (1986) evaluated a data set collected between the years 1982 to 1984 inclusive, at the Karlsruhe Nuclear Research Centre in Germany. Several buildings on the complex released gaseous tritium through stacks, but the most significant was the HWR which released 79% of the 142 TBq of gaseous tritium. The investigators used the ISOLA-III computer program to estimate the surface loading of tritium for rain and snow. They reported the concentrations of tritium in rain water and snow water to be approximately equal and their calculated results agreed closely with the measured results. This study did not specifically look at the interception coefficient for rain and snow; however, it contributes to this discussion by demonstrating an approximately equal concentration of tritium in rain run-off and snow melt.

Davis (1997) calculated both the dry deposition rate of HTO to snow and the washout coefficient of gaseous tritium by snow precipitation using a data set of tritium concentrations in snow compiled after an accidental release of tritium at the Chalk River plant in Canada. Davis (1997) calculated the dry deposition velocity of HTO to snow was $1.6 \times 10^{-3} \pm 0.5 \times 10^{-3}$ m s^{-1}. Additionally, he calculated the washout coefficient of

HTO by snow was $2.1x10^{-5} \pm 1.0x10^{-5}$ s^{-1}. Davis (1997) demonstrated the interception rate of tritium by snow was much lower than interception by rain.

Davis (1997) discussed the possibility of tritium accumulation in snow over the course of the winter with its subsequent release through melt in the spring. A large spring release could end up anywhere the melt goes, to include soil, soil water, incorporation into plants (such as crops), ground water (water table), aquifer, and surface water (streams, rivers, ponds, etc). Of importance to this discussion is the opinion of Davis (1997) that if HTO was released from the snow pack to the atmosphere, the emission rate would be low to negligible and that transfer of tritium in the environment during winter would be much slower than during summer. This opinion indicates the transfer rates of tritium in the environment should be highly dependent on the temperature of both the ambient air and the temperature of the medium.

Galeriu et al (2010) calculated the diffusion rate of tritium in the snow pack using the same data set as Davis (1997). Galeriu et al (2010) used computer aided calculations and compensated for environmental and weather conditions using downwind models to the extent practical. Galeriu et al (2010) found the diffusion coefficient of tritium in snow to be in the range 1×10^{-10} m^2s^{-1} to 2×10^{-10} m^2s^{-1} at 0^o C or below. The range is due to the diffusion of tritium in snow being subject to many environmental factors including temperature, the concentration of tritium in air, the presence of melt, the presence of the liquid phase melt around the individual particles of ice within the pack, the presence of air space within the pack, the density of the ice, and the spacial density of the snow and ice particles within the pack, etc. Galeriu et al (2010) reiterated what Davis (1997) published, that ambient temperature, and thus, snow pack temperature would greatly

impact the diffusion of tritium out of the pack. They also pointed out that fresh snow covering tritiated snow pack would help to isolate the tritiated layer and reduce losses to sublimation. Over time, throughout the winter, they measured an increasing density to the snow pack which they believed contributed to increased retention of tritium. They stated that approximately 70% of the initial tritium inventory was still present in the snow pack and contributed to HTO concentration in spring melt.

3. Methods and Materials

This project encompassed two objectives. The first objective was to determine the tritium interception rate by snow precipitation. The second objective was to determine the correlation, if any, between the spent fuel pool (SFP) tritium concentrations, tritium concentrations in the gaseous releases from Cook Nuclear Power Plant, and tritium concentrations in snow samples. Correlation between the tritium concentrations of the primary coolant loops of both units and the gaseous releases of tritium was also investigated.

3.1 Determination of Tritium Interception Rate

The interception rate of tritium released from Cook Nuclear Power Plant by snow precipitation was investigated. Data was obtained from several sources.

Tritium releases were calculated from data presented in the yearly Effluent Release Reports submitted to the United States Nuclear Regulatory Commission (NRC) by Cook Nuclear Power Plant. The tritium releases were reported to the NRC in total curies per calendar quarter. This data was converted to Bq s^{-1}, an average rate over the entire quarter. Tritium concentration in snow samples was reported in units of uCi mL^{-1}. Sample locations and sample dates were obtained from historical data sets of snow provided by the Cook Nuclear Power Plant Environmental Department. The snow tritium concentration data were converted to Bq cm^{-3}. Meteorological data was obtained from the weather station at the Southwest Michigan Regional Airport in Benton Harbor, MI as reported by Weather Underground (2016). The Southwest Michigan Regional Airport is approximately 14 miles north of Cook Nuclear Power Plant. The 10-m and 60-

m meteorological towers onsite could have provided wind speed and wind direction data but were not operating during key data collection times due to a broken instrument which was slated for repair. Meteorological data collected were wind speed in miles per hour converted to m s^{-1}, prevalent wind direction for each day, cloud cover, inches of snow deposited daily converted to cm, and the amount of time each snowfall lasted in hours converted to seconds. Relevant data ranged from 2008 to 2015.

The collection of the snow samples was performed by the Offsite Dose Coordinator, Cook Nuclear Power Plant Environmental Department. The collection was performed between 1 and 3 pm on the dates reported for each sample and were composited from the top one inch of snow in a six-inch by six-inch square. The approximate yield of melted snow from the collection was 50 mL.

The equation used to calculate the interception rate of tritium by snow precipitation was obtained from Davis (1997).

$$\Lambda = \frac{\sqrt{\frac{2}{\pi}} D_f C_f e^{\frac{-H^2}{2\sigma_z^2}}}{C_a \sigma_z \Delta t_f} \quad (1)$$

$$C_a = \frac{Q}{\pi u \sigma_y \sigma_z} e^{-\left(\frac{y^2}{2\sigma_y^2} + \frac{H^2}{2\sigma_z^2}\right)} \quad (2)$$

Λ = the interception rate in units of s^{-1}
D_f = the depth of falling snow collected during the storm in units of cm
C_f = the concentration of HTO in the sample in units of Bq cm^{-3}
H = the height above ground level of the release point in units of cm
Δt_f = the change in time from the start of the snow fall until the collection of the sample or end of the snow fall, in seconds, whichever is shorter
C_a = the concentration of HTO in air as given by Equation 2 in units of Bq cm^{-3}
σ_z = the lateral dispersion factor in units of cm
σ_y = the vertical dispersion factor in units of cm
Q = the emission rate of HTO from the stack in units of Bq s^{-1}

u = the mean wind speed in units of cm s^{-1}

y = the crosswind distance from the centerline of the plume to the point of collection in units of cm.

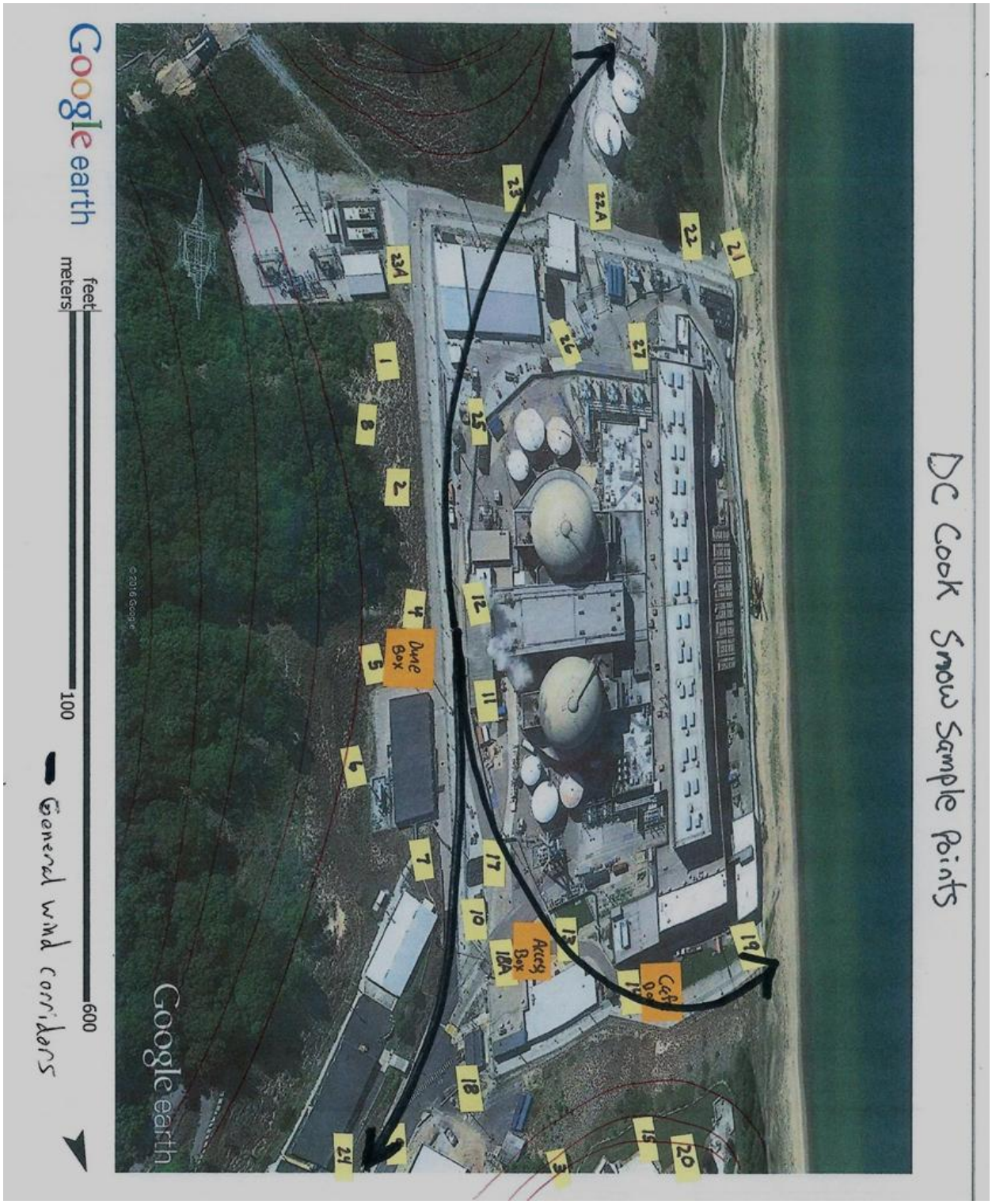

Figure 3. General wind corridors at Cook Nuclear Power Plant

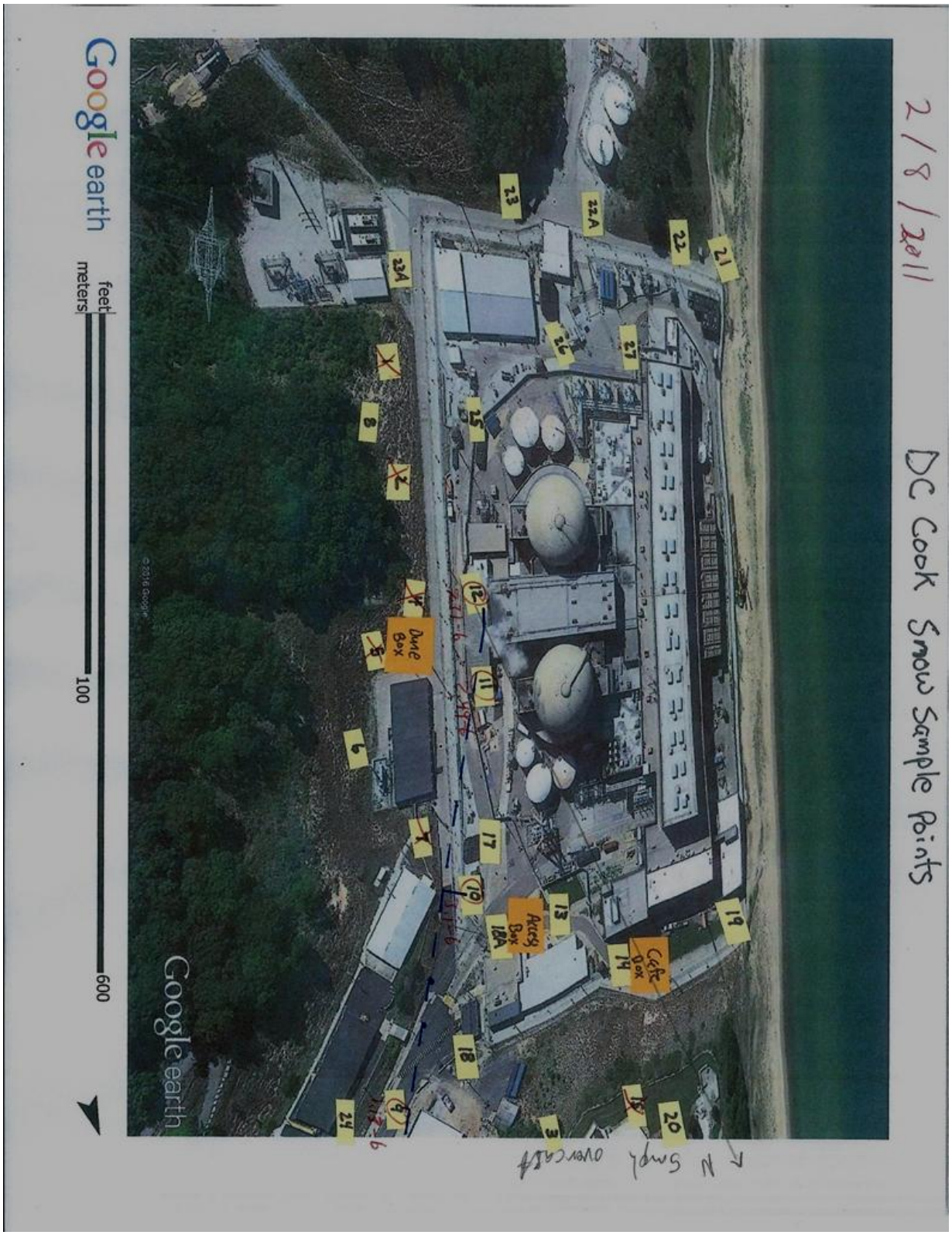

Figure 4. Typical Gaussian Plume centerline determination

The Gaussian Plume model variables of Equation 1, the vertical and horizontal dispersion factors, were obtained by referencing Gifford (1968). The collected meteorological data for each precipitation event was used to infer the Pasquill atmospheric stability class which in turn was used to infer the lateral and vertical dispersion factors. The Pasquill atmospheric stability class was obtained from Table 3.3, Relation of Turbulence Types to Weather Conditions, published in Gifford (1968) which uses the surface wind speed and relative cloud cover to obtain an atmospheric stability classification corresponding to the dispersion factor charts. The dispersion factors were inferred from Figures 3.10, Lateral Diffusion, and 3.11, Vertical Diffusion, published in Gifford (1968) which uses the downwind distance along the centerline of the plume along with the Pasquill atmospheric stability class to obtain the appropriate dispersion factor.

The downwind distance and crosswind distances were determined by creating scale maps of the complex for each sampling period annotated with each collection point sampled on that date and its corresponding tritium concentration result from sampling. The wind direction onsite was affected by building wake and the presence of large sand dunes and as a result the wind direction reported by the airport was obviously not the effective wind direction at the complex. Information gathered from the Cook Nuclear Power Plant Environmental Department indicated three general wind corridors existed on site (see Figure 3). The pattern of sampling, the points selected by the Environmental Department for sampling after each snowfall, was generally a reflection of the onsite wind direction for the specific event. Therefore, the sample results were used in conjunction with the indicated wind corridors to estimate an effective wind direction, or plume center line, from which downwind distance and crosswind distance could be

estimated and measured (see Figure 4). While not ideal, this method was the only method of determining effective wind direction given that site-specific meteorological data was not available for the precipitation events investigated.

3.2 Determination of Correlation Between Data

Correlation between the spent fuel pool (SFP) tritium concentrations, tritium concentrations in the gaseous releases from Cook Nuclear Power Plant, and tritium concentrations in snow samples was investigated. Correlation between the tritium concentrations of the primary coolant loops of both units and the gaseous releases of tritium was also investigated.

Data on gaseous tritium releases and snow concentrations of tritium were already available from the analysis of the tritium interception rate. The tritium concentrations of the spent fuel pool and both primary coolant loops were obtained from the Cook Nuclear Power Plant Environmental Department in the form of a graphic (see Figure 5).

To compare the three data sets, the data in Table 1 was organized by calendar quarter, to match the lowest resolution data set, the gaseous releases of tritium. In order to make the three data sets relatable, the snow concentrations, SFP concentrations, and cooling loop concentrations were modified to represent average quarterly data. Gaseous tritium release data were not available for the year 2015 at the time of this study. The three data points in Table 1 marked with an "*" were imputed using regression analysis and a linear model fit on the SFP and cooling loop concentration data.

The SFP/cooling loop data graph (Figure 5) was busy with large variation within single calendar quarters making determination of quarterly concentration difficult. The

blue data points represent the tritium concentration of the spent fuel pool. The red and green data points represent the tritium concentrations of the Unit 1 and Unit2 cooling systems respectively. The data over entire quarters could not be averaged because the raw data points were not available. Therefore, an approximate average for each quarter was estimated from the graph.

The snow concentration data were available and aggregated into quarterly averages. Data reported as below the Lower Limit of Detection (LLD) were assigned a half-value of the quoted LLD.

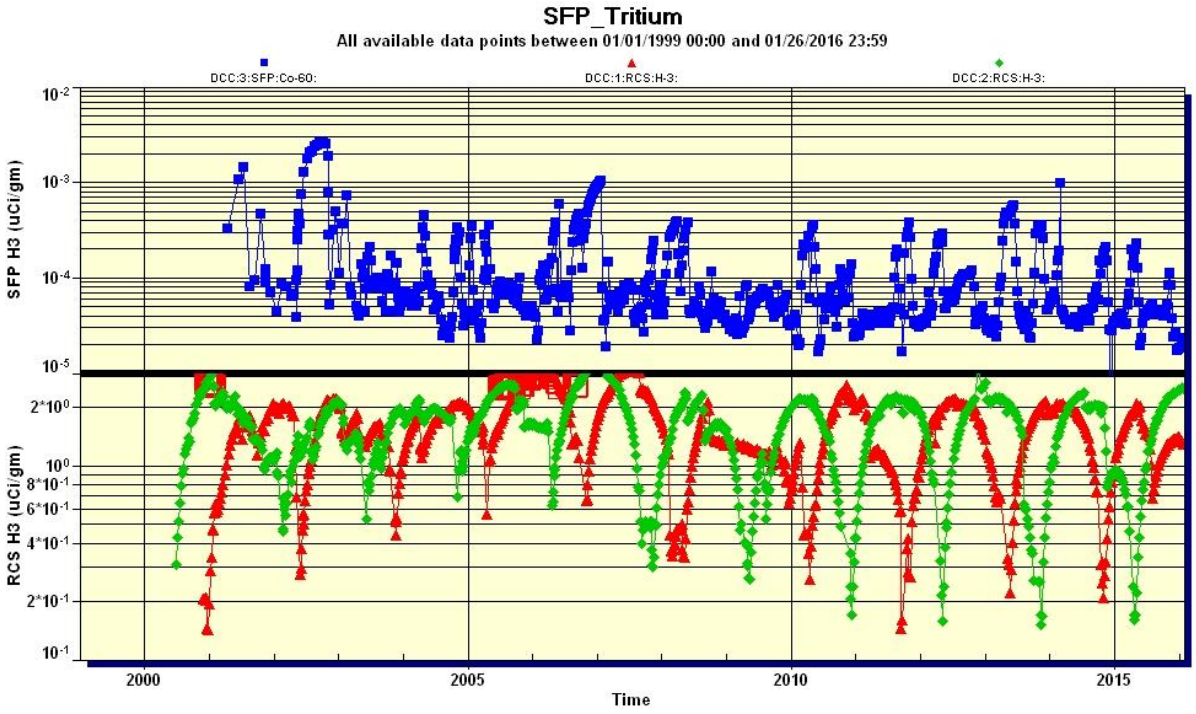

Figure 5. Cook Nuclear Power Plant SFP and Units 1 & 2 tritium concentrations over time

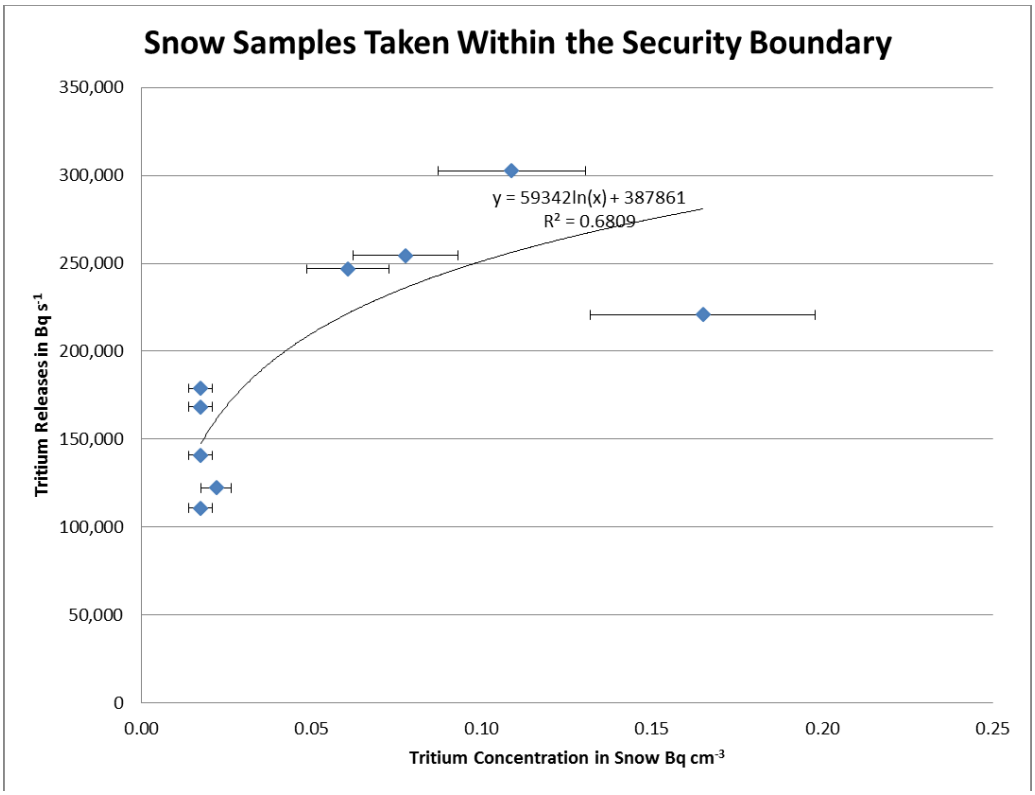

Figure 6. Snow sample data graphed against tritium release data

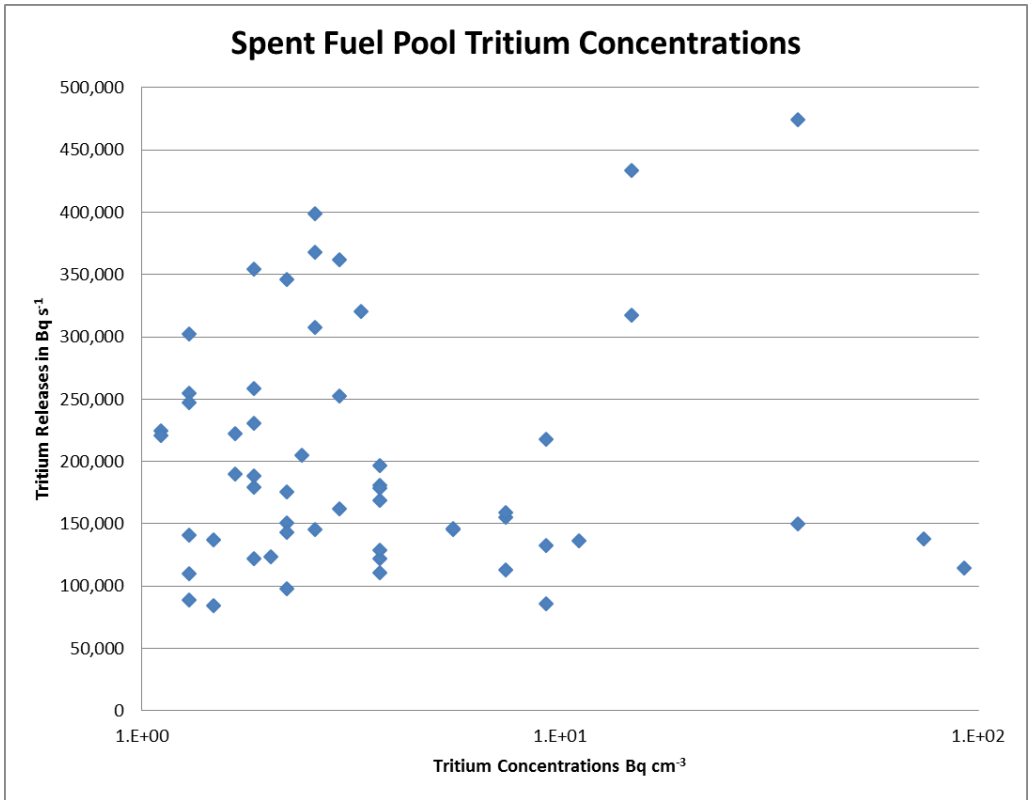

Figure 7. Spent fuel pool concentration data graphed against tritium release data

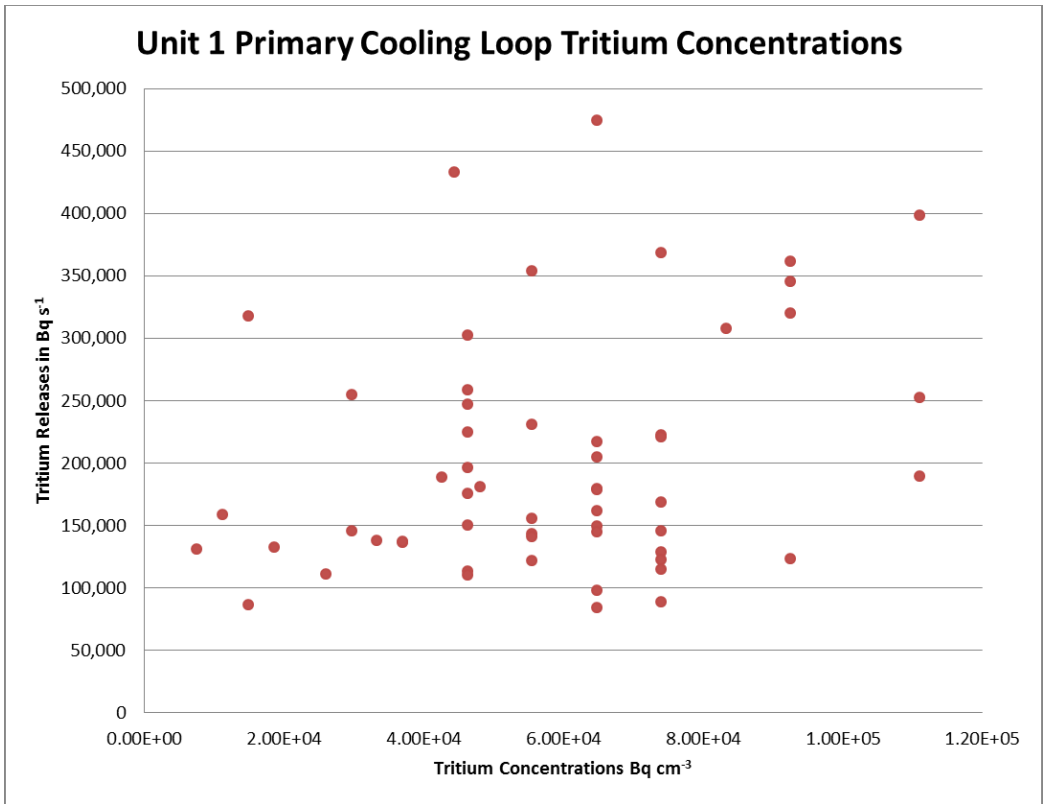

Figure 8. Unit 1 concentration data graphed against tritium release data

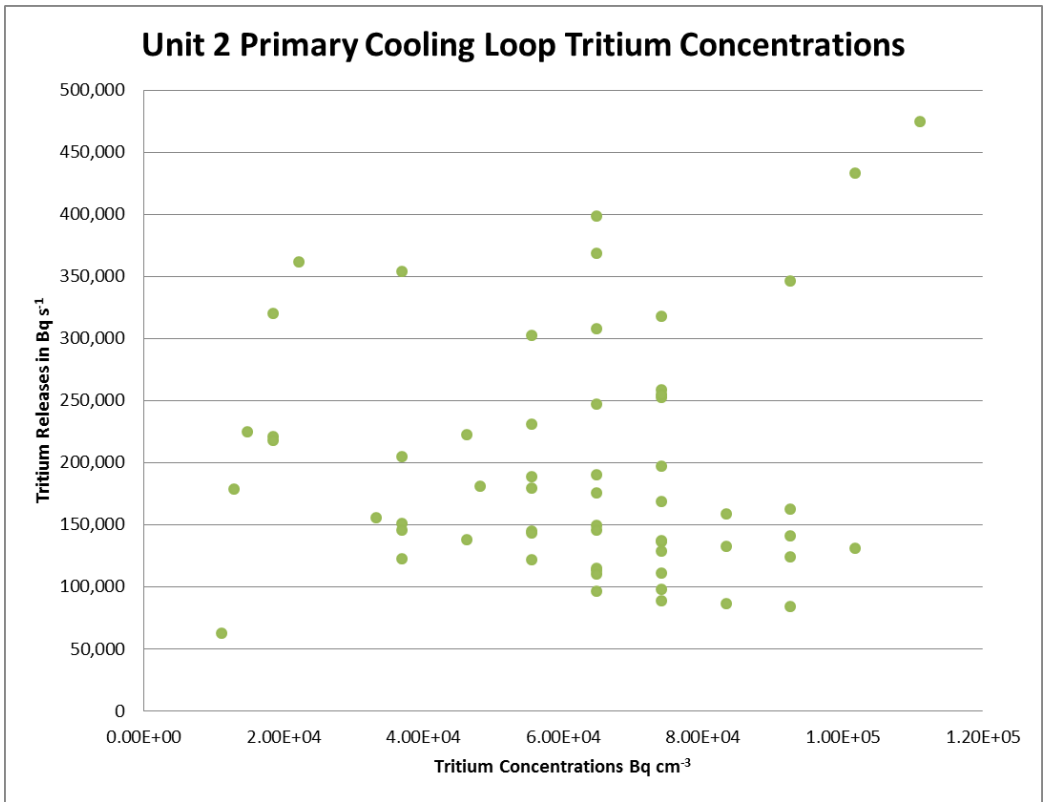

Figure 9. Unit 2 concentration data plotted against tritium release data

The SFP/cooling loop data were plotted against the gaseous release data and the gaseous release data were plotted against the snow sample concentration data (see Figures 6-9). The snow sample data graphed against tritium release data was further analyzed for trends by fitting an exponential trend line to the data (see Figure 6). A regression analysis was conducted across all data sets presented in Table 1. Data from snow sample points 4, 10, 11, 12, 13, and 18 were chosen for correlation with the gaseous tritium release data because those points had the greatest number of samples and the greatest number of positive results available to conduct a meaningful analysis.

4. Results and Discussion

4.1 Determination of Tritium Interception Rate

Determination of the potential error in the meteorological data used was made by calculating the correlation between the meteorological data used by Hinchcliffe (2010) in his study of rain interception rate. Hinchcliffe was able to obtain meteorological data from the towers at Cook Nuclear Power Plant. Hinchcliffe's meteorological data was matched to data from the Southwest Michigan Regional Airport for the dates available. A correlation was calculated for a total of 292 data points of wind speed and wind direction. The calculated correlation for the wind speed data was 0.71 indicating a moderate probability of correlation. The calculated correlation for the wind direction data was 0.57 indicating a low probability of correlation. This result leads to the conclusion that the wind speed data is usable but the wind direction data does not represent the study site and an alternative method for determining wind direction is necessary. Based upon the greatest delta between the two data sets, the potential error in the wind speed data could be as great as 50% and the potential error in the wind direction data could be as much as 100%.

The model used to calculate the tritium interception rate by snow, Equation 1, is very sensitive to changes in meteorological factors because it is a variation of the Gaussian Plume model. Eighteen calculated interception rate data points were immediately identified as potential outliers. One example was a point yielding a result of 7.46×10^{37} s^{-1} unlike the median value of 1.51×10^{-6} s^{-1}. Examination of the scale maps from which the downwind distance and crosswind distances were derived revealed that

each suspected outlier was much further off the plume centerline than any other point for that particular precipitation event, and was most probably the result of wind direction changes during the storm. The average crosswind distance was determined to be 21 meters for all points. The average crosswind distance for the outliers was 65 meters. The average crosswind distance was 8 meters with all suspected outliers eliminated. This variation was expected given the turbulent meteorological conditions and microclimate of the complex. Stated another way, due to the meteorological conditions at the site, it is unlikely all points for any given precipitation event are the result of one specific plume centerline. This is a disadvantage of the Gaussian Plume model, as it cannot account for such variation. The eighteen outliers were eliminated from the data and the remaining points plotted (see Figure 10). The results of the tritium interception rate calculations are given in Table 2. The observed variation in the graph can likely be attributed to variation and instability in the meteorology of the site; however, there is an overwhelming grouping of plotted points which a frequency plot illustrates.

A frequency plot of the points presented in Figure 10 was created (see Figure 11). The frequency plot demonstrates that 49% of the data points fall between $1x10^{-6}$ s^{-1} and $1x10^{-7}$ s^{-1} and an additional 28% of the data points fall between $1x10^{-5}$ s^{-1} and $1x10^{-6}$ s^{-1}.

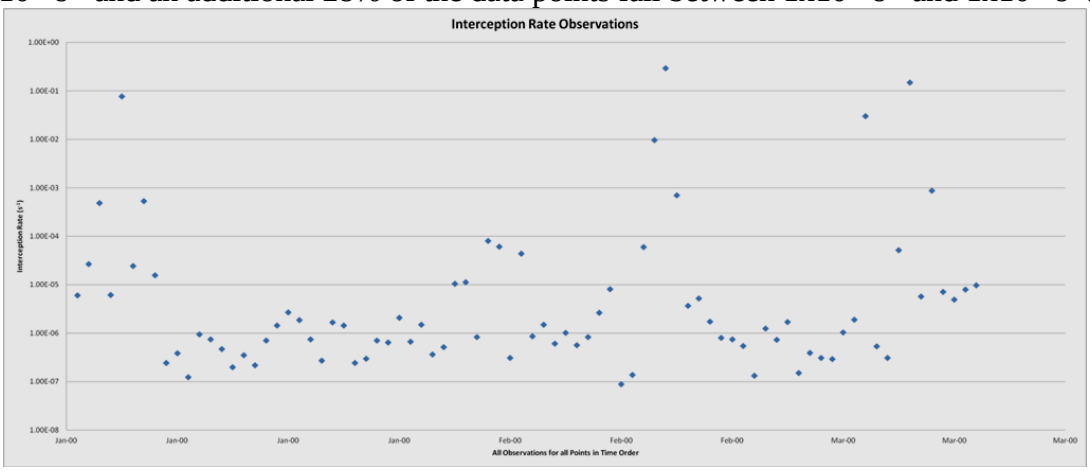

Figure 10. All calculated tritium interception rate observations

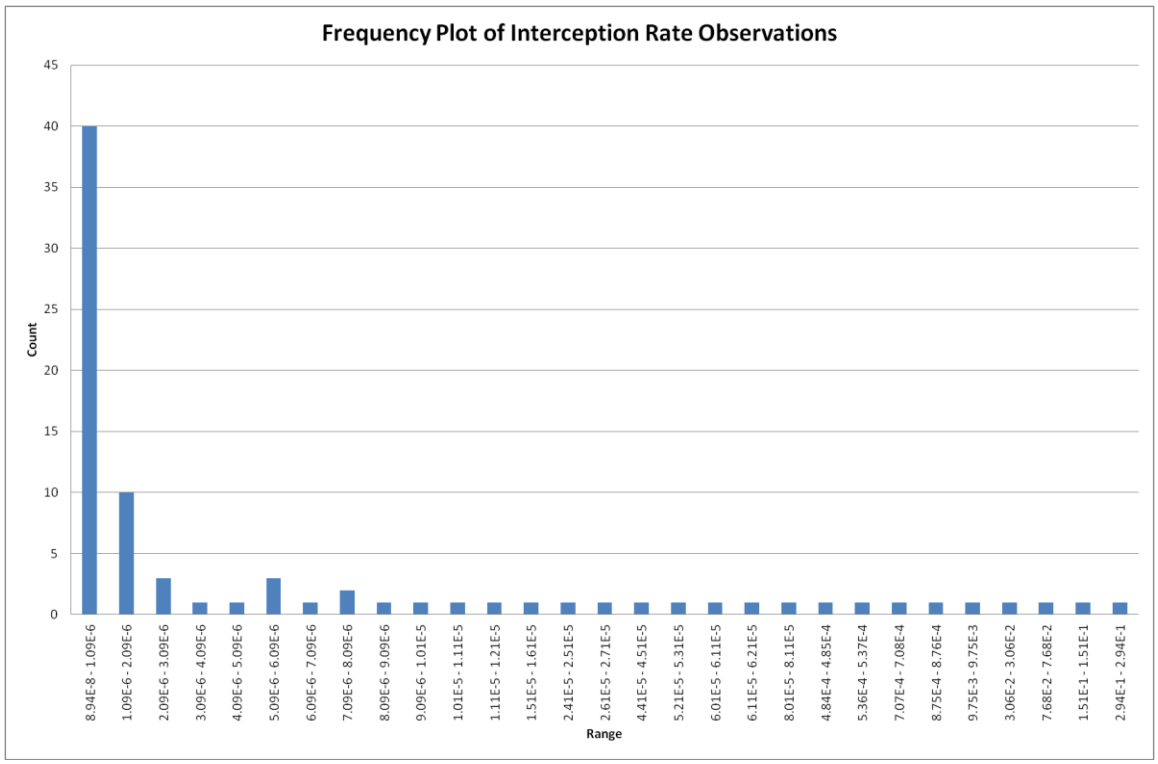

Figure 11. Frequency plot of interception rate observations

These results differ moderately from Davis (1997) who calculated the interception rate of tritium by snow to be $2.1 \times 10^{-5} \pm 1.0 \times 10^{-5}$ s^{-1}. The results of this study indicate the interception rate for the conditions tested is likely between 1×10^{-5} s^{-1} and 1×10^{-7} s^{-1}. Several differences between the studies are noted. First, the amount of tritium released at Chalk River during the incident from which the data set utilized by Davis (1997) was created was about 700 TBq over the course of 18 days. The highest tritium release during a winter quarter at the Cook Nuclear Power Plant was 3.7 TBq over the entire 90 days. Second, the Chalk River facility was able to gather reliable meteorological data directly from the site, including wind direction, wind speed, etc. Third, the Davis (1997) study used computer-aided meteorological models which accounted for turbulence and

compensated for building wake in the calculations. These factors alone undoubtedly play a significant role in the difference between the two calculated interception rates.

4.2 Determination of Correlation Between Data

The SFP/cooling loop data were plotted against the gaseous release data and the gaseous release data were plotted against the snow sample concentration data (see Figures 6-9). The statistical software package R was used to conduct a regression analysis of all data sets. Results are given in Table 3. Only nine matching data points were available for the regression analysis. A linear regression model was fit to all matching data points from the SFP, Unit 1, and Unit 2 as predictors of the release data. Using the model, three data points were imputed for Quarter 1 of 2015, Quarter 4 of 2015, and Quarter 1 of 2016. The regression analysis was redone with the 9 original data points and the three additional imputed data points. Results are given in Table 4. Results indicated no correlation between any of the data sets and tritium concentrations in snow samples. The p-values reported by the analysis did not meet the criteria of being less than 0.05. The trend line fitted to the graph of gaseous tritium releases and tritium concentrations in snow presented in Figure 6 had a calculated R^2 value of 0.68 indicating a low probability of correlation. The correlation was calculated between the gaseous releases and each of the six data points chosen. The highest value returned was 0.627 for point 12, indicating a low probability of correlation.

5. Conclusions

5.1 Determination of Tritium Interception Rate

The tritium interception rate by snow precipitation at Cook Nuclear Power Plant likely falls within the range between $1x10^{-5}$ s^{-1} and $1x10^{-7}$ s^{-1} for the conditions at the site. This result reflects the fact that large averages of data were used to calculate results which were actually created by varying conditions during discrete events over the period of the averages. Low resolution tritium release data and lack of site-specific meteorological data significantly impacted the results of this analysis making the determination of high resolution interception rates impossible.

5.2 Determination of Correlation Between Data

Analysis of the available data showed no correlation between tritium concentrations in either of the individual unit cooling systems to the tritium releases. Analysis also showed no correlation between the spent fuel pool tritium concentrations and the tritium releases. Also, no correlation was established between the tritium releases and the snow concentrations of tritium. The low releases of tritium from Cook Nuclear Power Plant may be insufficient to show strong correlation between the data sets. The low resolution of the data was not ideal for the analysis. It may yet be possible to draw useful conclusions from a future analysis when high resolution data is made available.

5.3 Future Research

The single greatest problem that needs to be overcome is the lack of resolution within the data. The data simply cannot support conclusions at the level desired by this project. Overarching 90-day averages of data do not have the resolution to draw conclusions about events happening on one particular day under a particular set of environmental conditions. Future research will need day-to-day meteorological data for the specific precipitation events being analyzed. Hour by hour data would be ideal. Quarterly averages of tritium releases are not sufficient. The actual tritium releases for the specific dates of the precipitation events are needed. Tritium release concentrations over long periods are needed in order to show correlation with other systems and events such as snow tritium concentrations. Quarterly tritium concentrations from the systems within the power plant are not sufficient. Tritium concentrations from each primary cooling loop and the spent fuel pool over long periods of time are needed to show correlation. Without high resolution data, this project simply will not be capable of returning useful results that possess small margins of error. This project may need to be done at a facility with more significant tritium releases and fewer security and environmental concerns than Cook Nuclear Power Plant.

A future analysis of tritium behavior in the snow pack could still be possible with the collection boxes. The collection and sampling method may need to be modified to account for security concerns on the site and efficiency of sampling. Also, the data collection may need to continue for several winter seasons before sufficient data is available to conduct an analysis.

References

Allen, Durrenberger. CHE357: Gaussian Plume Modeling. Austin: University of Texas; 2015.

Ahmed SN. Physics & engineering of radiation detection. San Diego: Academic Press; 2007.

Baum EM, Knox HD, Miller TR. Nuclides and isotopes: chart of the nuclides, 16th ed. Niskayuna: KAPL; 2002.

Cember H, Johnson TE. Introduction to Health Physics, 4th ed. New York: McGraw Hill; 2009.

Chi CL, Jiunn-Hsing C, Chien CL. Tritium release from nuclear power plants in Tiawan. Health Physics 84(3):361-367; 2003. DOI:0017-9078/03/0

Davis PA. Tritium transfer parameters for the winter environment. Journal of Environmental Radioactivity 36(2-3):177-196; 1997. DOI:0265-931X/97

Eisenbud M, Gesell T. Environmental Radioactivity, 4th ed. San Diego: Academic Press; 1997.

Galeriu D, Davis P, Workman W. Tritium profiles in snowpacks. Journal of Environmental Radioactivity 101:869-874; 2010. DOI:10.1016/j.jenvrad.2010.05.013

Gifford F. An outline of theories of diffusion in the lower layers of the atmosphere. In: Slade DH, ed. Meteorology and atomic energy. Springfield, VA: National Technical Information Service; 1968: 65-116.

Harris J. HPHY 6605: Radiological Environmental Monitoring and Surveillance. Pocatello: Idaho State University Health Physics Department; 2015.

Harris JT, Miller DW, Foster DW. Tritium recapture behavior at a nuclear power reactor due to airborne releases. Health Physics 95(2):203-212; 2008. DOI:0017-9078/08/0

Hinchcliffe W. Investigation of tritium recapture at Cook Nuclear Power Plant from airborne effluent releases. Pocatello, ID: Idaho State University; 2010. Thesis.

Jacobs DG. Sources of tritium and its behavior upon release to the environment. AEC Critical Review Series. 1968.

Lederer CM, Shirley VS, Browne E, Dairiki JM, Doebler RE, Shihab-Eldin AA, Jardine LJ, Tuli JK, Buyrn AB. Table of isotopes, 7th ed. New York: Wiley & Sons; 1978.

Luykx F, Fraser G. Tritium releases from nuclear power plants and nuclear fuel reprocessing plants. Radiation Protection Dosimetry 16(1-2):31-36; 1986.

Martin JE. Physics for radiation protection, 3rd ed. Hoboken: Wiley & Sons; 2013.

Monterrosa A, Iyengar A, Huynh A, Madaan, C. Department of Nuclear Engineering. Boron use and control in PWRs and FHRs. University of California, Berkeley; Report UCBTH-12-007; 2012.

Nuclear Energy Institute. U.S. Nuclear Power Plants [online]. Washington, DC: NEI 2015. Available at: http://www.nei.org/Knowledge-Center/Nuclear-Statistics/US-Nuclear-Power-Plants Accessed 19 September 2015.

Papadopoulos D, Konig LA, Langguth KG, Fark S. Contamination of precipitation due to tritium release into the atmosphere. Radiation Protection Dosimetry 16(1-2):95-100; 1986.

R Core Team. R: A language and environment for statistical computing. R Foundation for Statistical Computing. Vienna, Austria; 2016. Available at: https://www.R-project.org/.

Shleien B. The health physics and radiological health handbook, revised ed. Silver Spring: Scinta, Inc; 1992.

Siemer D. NE 5551: Seminar, Why the molten salt fast reactor (MSFR) is the "best" GEN-IV reactor. Pocatello: Idaho State University Health Physics Department; 2014.

The Virtual Nuclear Tourist. Pressurized Water Reactor (PWR) [online]. Available at: http://www.nucleartourist.com/type/pwr.htm. Accessed 8 Apr 2016.

Tsoulfanidis N, Landsberger S. Measurement and detection of radiation, 3rd ed. Boca Raton: CRC Press; 2011.

Turner JE. Atoms, radiation and radiation protection, 2nd ed. New York: Wiley & Sons; 1995.

US Nuclear Regulatory Commission. Boiling water reactors [online]. Available at: http://www.nrc.gov/reactors/bwrs.html. Accessed 12 April 2016.

US Nuclear Regulatory Commission. Pressurized water reactors [online]. Available at: http://www.nrc.gov/reactors/pwrs.html. Accessed 12 April 2016.

Weather Underground. Benton Harbor, MI [online]. Available at: https://www.wunderground.com/history/airport/KBEH/2016/04/08/DailyHistory.html?req_city=Bridgman&req_state=MI&reqdb.zip=49106&reqdb.magic=1&reqdb.wmo=99999. Accessed 8 April 2016.

World Nuclear Association. Lithium [online]. Available at: http://www.world-nuclear.org/information-library/current-and-future-generation/lithium.aspx. Accessed 8 April 2016.

World Nuclear Association. Plutonium [online]. Available at: http://www.world-nuclear.org/information-library/nuclear-fuel-cycle/fuel-recycling/plutonium.aspx. Accessed 8 April 2016.

Appendix A. Data Tables

Table 1. Comparative chart of all three data sets

	Tritium Concentrations Bq/cm^3			Releases Bq/s	Avg Snow Samples Bq/cm^3	
Quarter	SFP	DCC 1 RCS	DCC 2 RCS	gaseous tritium	All Samples	Near Facility
Jan-99				119431.58		
Apr-99				92384.52		
Jul-99				67844.88		
Oct-99				80889.92		
Jan-00				134657.92		
Apr-00				105376.09		
Jul-00			1.11E+04	62552.02		
Oct-00			6.48E+04	96116.26		
Jan-01		7.40E+03	1.02E+05	130851.34		
Apr-01	1.11E+01	3.70E+04	7.40E+04	136652.10		
Jul-01	3.70E+01	6.48E+04	6.48E+04	149643.67		
Oct-01	3.70E+00	5.55E+04	5.55E+04	121810.70		
Jan-02	1.67E+00	7.40E+04	4.63E+04	222209.36		
Apr-02	2.41E+00	6.48E+04	3.70E+04	204978.15		
Jul-02	7.40E+01	3.33E+04	4.63E+04	138095.61		
Oct-02	9.25E+01	7.40E+04	6.48E+04	114673.35		
Jan-03	3.70E+00	7.40E+04	7.40E+04	128472.22		
Apr-03	1.85E+00	6.48E+04	5.55E+04	179476.18		
Jul-03	7.40E+00	5.55E+04	3.33E+04	155417.71		
Oct-03	3.70E+00	4.81E+04	4.81E+04	180812.76		
Jan-04	2.22E+00	4.63E+04	6.48E+04	175578.70		
Apr-04	7.40E+00	4.63E+04	6.48E+04	113074.80		
Jul-04	2.22E+00	6.48E+04	7.40E+04	97677.38		
Oct-04	2.59E+00	7.40E+04	6.48E+04	368287.04		
Jan-05	5.55E+00	6.48E+04	5.55E+04	145126.03		
Apr-05	3.70E+00	4.63E+04	7.40E+04	196798.27		
Jul-05	2.96E+00	6.48E+04	9.25E+04	162154.08		
Oct-05	2.04E+00	9.25E+04	9.25E+04	123713.99		
Jan-06	1.67E+00	1.11E+05	6.48E+04	189853.40		
Apr-06	2.59E+00	1.11E+05	6.48E+04	398889.41		
Jul-06	2.59E+00	8.33E+04	6.48E+04	307948.40		
Oct-06	1.48E+01	4.44E+04	1.02E+05	433474.79		
Jan-07	3.70E+01	6.48E+04	1.11E+05	474395.58		
Apr-07	2.22E+00	9.25E+04	9.25E+04	345960.78		
Jul-07	2.96E+00	1.11E+05	7.40E+04	252613.92		
Oct-07	3.33E+00	9.25E+04	1.85E+04	320228.91		
Jan-08	1.85E+00	5.55E+04	3.70E+04	354012.35	1.69E-02	
Apr-08	1.48E+01	1.48E+04	7.40E+04	317571.79		
Jul-08	1.85E+00	4.63E+04	7.40E+04	258869.12		
Oct-08	1.85E+00	5.55E+04	5.55E+04	230774.18		
Jan-09	1.30E+00	4.63E+04	5.55E+04	302623.46	7.67E-02	1.09E-01
Apr-09	1.11E+00	4.63E+04	1.48E+04	224706.10		
Jul-09	2.22E+00	4.63E+04	3.70E+04	150606.01		
Oct-09	1.85E+00	4.26E+04	5.55E+04	188425.93		
Jan-10	1.30E+00	2.96E+04	7.40E+04	254565.33	7.06E-02	7.76E-02
Apr-10	9.25E+00	1.48E+04	8.33E+04	86129.32		
Jul-10	2.22E+00	5.55E+04	5.55E+04	143388.47		
Oct-10	2.96E+00	9.25E+04	2.22E+04	361625.51		
Jan-11	1.11E+00	7.40E+04	1.85E+04	220781.89	1.48E-01	1.65E-01
Apr-11	1.30E+00	4.63E+04	6.48E+04	110187.79		
Jul-11	1.48E+00	3.70E+04	7.40E+04	137133.27		
Oct-11	7.40E+00	1.11E+04	8.33E+04	158924.90		
Jan-12	1.30E+00	4.63E+04	6.48E+04	246952.16	3.57E-02	6.06E-02
Apr-12	9.25E+00	6.48E+04	1.85E+04	217488.56		
Jul-12	2.59E+00	7.40E+04	3.70E+04	145313.15		
Oct-12	3.70E+00	7.40E+04	7.40E+04	168441.36	1.74E-02	1.74E-02
Jan-13	1.30E+00	5.55E+04	9.25E+04	140843.62	3.07E-02	1.74E-02
Apr-13	9.25E+00	1.85E+04	8.33E+04	132802.75		
Jul-13	5.55E+00	2.96E+04	6.48E+04	145794.32		
Oct-13	3.70E+00	6.48E+04	1.30E+04	178909.47	2.90E-02	1.74E-02
Jan-14	1.85E+00	7.40E+04	3.70E+04	122286.52	2.25E-02	2.20E-02
Apr-14	1.30E+00	7.40E+04	7.40E+04	89016.33		
Jul-14	1.48E+00	6.48E+04	9.25E+04	84204.64		
Oct-14	3.70E+00	2.59E+04	7.40E+04	110866.77	1.74E-02	1.74E-02
Jan-15	1.30E+00	3.33E+04	3.33E+04	*168605	6.49E-02	8.90E-02
Apr-15	3.70E+00	6.48E+04	1.48E+04			
Jul-15	1.67E+00	5.55E+04	5.55E+04			
Oct-15	1.67E+00	4.63E+04	7.40E+04	*191921	1.74E-02	1.74E-02
Jan-16	7.40E-01	5.55E+04	9.25E+04	*206383	6.89E-02	8.34E-02

Table 2. Tritium interception rate calculation results

Date	RG#	Λ s^{-1}	D_f cm	C_f uCi/mL	C_f Bq/cm^3	H cm	Δt_f s	C_a Bq/cm^3	σ_x cm	Q Bq/s	u m/s	σ_y m	y m	σ_z m	H m	downwind distance (m)	stability class
2/9/2009	9	6.05E-06	0.559	1.19E-06	4.40E-02	4500	9660	5.69E-30	410	302623	2.7	7.5	6.25	4.1	45	134	E
2/9/2009	18	2.69E-05	0.559	5.39E-06	1.99E-01	4500	9660	2.81E-31	400	302623	2.7	7	6.25	4	45	120	E
2/9/2009	24	4.85E-04	0.559	9.60E-07	3.55E-02	4500	9660	1.45E-27	450	302623	2.7	8	25	4.5	45	143	E
2/11/2009	7	6.22E-06	3.124	1.04E-06	3.85E-02	4500	39720	3.85E-22	490	302623	3.1	8	0	4.9	45	62.5	D
2/11/2009	15	7.68E-02	3.124	1.94E-06	7.18E-02	4500	39720	1.43E-24	510	302623	3.1	9	37.5	5.1	45	106.25	D
2/11/2009	18	2.47E-05	3.124	2.80E-06	1.04E-01	4500	39720	1.39E-18	550	302623	3.1	9.5	6.25	5.5	45	118.75	D
2/11/2009	18A	5.37E-04	3.124	5.76E-06	2.13E-01	4500	39720	2.05E-126	190	302623	3.1	8	18.75	1.9	45	81.25	D
2/16/2009	4	1.58E-05	0.076	1.01E-06	3.74E-02	4500	21180	2.45E-41	350	302623	1.8	6	18.75	3.5	45	6.25	E
2/16/2009	7	2.45E-07	0.076	1.20E-06	4.44E-02	4500	21180	1.88E-39	350	302623	1.8	6	6.25	3.5	45	62.5	E
2/16/2009	12	3.84E-07	0.076	1.88E-06	6.96E-02	4500	21180	1.88E-39	350	302623	1.8	6	6.25	3.5	45	0	E
2/16/2009	13	1.24E-07	0.076	1.04E-06	3.85E-02	4500	21180	3.24E-39	350	302623	1.8	6	0	3.5	45	87.5	E
2/16/2009	25	9.54E-07	0.076	8.03E-06	2.97E-01	4500	21180	3.24E-39	350	302623	1.8	6	0	3.5	45	50	E
2/3/2010	9	7.44E-07	0.102	3.54E-06	1.31E-01	4500	48480	3.01E-16	600	254565	2.2	10.4	6.25	6	45	137.5	D
2/3/2010	10	4.78E-07	0.102	2.61E-06	9.66E-02	4500	48480	3.36E-22	490	254565	2.2	8	6.25	4.9	45	75	D
2/3/2010	11	2.01E-07	0.102	1.49E-06	5.51E-02	4500	48480	4.56E-22	490	254565	2.2	8	0	4.9	45	18.75	D
2/3/2010	12	3.53E-07	0.102	1.93E-06	7.14E-02	4500	48480	3.36E-22	490	254565	2.2	8	6.25	4.9	45	0	D
2/3/2010	14	2.20E-07	0.102	1.45E-06	5.37E-02	4500	48480	9.97E-21	510	254565	2.2	9	0	5.1	45	112.5	D
2/3/2010	17	7.10E-07	0.102	3.88E-06	1.44E-01	4500	48480	3.36E-22	490	254565	2.2	8	6.25	4.9	45	62.5	D
2/3/2010	18	1.46E-06	0.102	7.32E-06	2.71E-01	4500	48480	7.60E-21	510	254565	2.2	9.5	6.25	5.1	45	118.75	D
2/3/2010	18A	2.71E-06	0.102	5.92E-06	2.19E-01	4500	48480	1.34E-22	490	254565	2.2	8	12.5	4.9	45	87.5	D
2/11/2010	12	1.88E-06	0.635	1.59E-06	5.88E-02	4500	95340	1.64E-22	490	254565	4.5	8	6.25	4.9	45	0	D
2/17/2010	11	7.55E-07	0.406	3.64E-06	1.35E-01	4500	176820	3.23E-22	490	254565	3.1	8	0	4.9	45	18.75	D
2/17/2010	12	2.74E-07	0.406	9.73E-07	3.60E-02	4500	176820	2.38E-22	490	254565	3.1	8	6.25	4.9	45	0	D
2/17/2010	13	1.68E-06	0.406	8.09E-06	2.99E-01	4500	176820	3.23E-22	490	254565	3.1	8	0	4.9	45	87.5	D
2/17/2010	14	1.44E-06	0.406	6.17E-06	2.28E-01	4500	176820	7.07E-21	510	254565	3.1	9	0	5.1	45	112.5	D
2/17/2010	17	2.45E-07	0.406	8.71E-07	3.22E-02	4500	176820	2.38E-22	490	254565	3.1	8	6.25	4.9	45	62.5	D
2/18/2010	9	2.98E-07	0.406	1.09E-06	4.03E-02	4500	182220	1.03E-25	450	254565	3.1	8	6.25	4.5	45	137.25	E
2/18/2010	10	7.04E-07	0.406	2.71E-06	1.00E-01	4500	182220	9.20E-40	350	254565	3.1	6	6.25	3.5	45	75	E
2/18/2010	11	6.43E-07	0.406	4.26E-06	1.58E-01	4500	182220	1.58E-39	350	254565	3.1	6	0	3.5	45	18.75	E
2/18/2010	12	2.11E-06	0.406	8.11E-06	3.00E-01	4500	182220	9.20E-40	350	254565	3.1	6	6.25	3.5	45	0	E
2/18/2010	14	6.69E-07	0.406	4.09E-06	1.51E-01	4500	182220	3.74E-34	380	254565	3.1	6.5	0	3.8	45	106.25	E
2/18/2010	17	1.50E-06	0.406	5.78E-06	2.14E-01	4500	182220	9.20E-40	350	254565	3.1	6	6.25	3.5	45	56.25	E
2/18/2010	18	3.65E-07	0.406	1.39E-06	5.14E-02	4500	182220	2.06E-31	400	254565	3.1	7	6.25	4	45	118.75	E
2/18/2010	20	5.18E-07	0.406	2.42E-06	8.95E-02	4500	182220	5.27E-23	480	254565	3.1	8.5	0	4.8	45	150	E
2/18/2010	24	1.06E-05	0.406	3.37E-06	1.25E-01	4500	182220	8.98E-27	450	254565	3.1	8	18.75	4.5	45	143.75	E
2/19/2010	1	1.13E-05	0.406	8.58E-06	3.17E-01	4500	182220	1.81E-40	350	254565	3.1	6	12.5	3.5	45	75	E
2/19/2010	2	8.30E-07	0.406	5.50E-06	2.04E-01	4500	182220	1.58E-39	350	254565	3.1	6	0	3.5	45	43.75	E
2/19/2010	4	8.05E-05	0.406	4.04E-06	1.49E-01	4500	182220	1.20E-41	350	254565	3.1	6	18.75	3.5	45	6.25	E
2/19/2010	5	6.18E-05	0.406	3.10E-06	1.15E-01	4500	182220	1.20E-41	350	254565	3.1	6	18.75	3.5	45	25	E
2/19/2010	6	3.09E-07	0.406	1.19E-06	4.40E-02	4500	182220	9.20E-40	350	254565	3.1	6	6.25	3.5	45	50	E
2/19/2010	7	4.44E-05	0.406	2.23E-06	8.25E-02	4500	182220	1.20E-41	350	254565	3.1	6	18.75	3.5	45	56.25	E
2/19/2010	8	8.74E-07	0.406	5.79E-06	2.14E-01	4500	182220	1.58E-39	350	254565	3.1	6	0	3.5	45	62.5	E
2/19/2010	23	1.51E-06	0.406	8.57E-06	3.17E-01	4500	182220	3.07E-31	400	254565	3.1	7	0	4	45	118.75	E
3/3/2010	9	6.15E-07	0.381	1.29E-06	4.77E-02	4500	105960	2.26E-16	600	254565	3.5	10.4	0	6	45	137.5	D
3/3/2010	11	1.03E-06	0.381	2.81E-06	1.04E-01	4500	105960	2.87E-22	490	254565	3.5	8	0	4.9	45	18.75	D
3/3/2010	13	5.65E-07	0.381	1.54E-06	5.70E-02	4500	105960	2.87E-22	490	254565	3.5	8	0	4.9	45	87.5	D
3/3/2010	17	8.31E-07	0.381	1.67E-06	6.18E-02	4500	105960	2.11E-22	490	254565	3.5	8	6.25	4.9	45	56.25	D
3/3/2010	18	2.65E-06	0.381	8.69E-07	3.22E-02	4500	105960	1.84E-19	550	254565	3.5	9.5	18.75	5.5	45	118.75	D
3/3/2010	18A	8.12E-06	0.381	1.42E-06	5.25E-02	4500	105960	1.84E-23	490	254565	3.5	8	18.75	4.9	45	75	D
1/21/2011	1	8.94E-08	0.431	5.99E-06	2.22E-01	4500	82620	1.02E-20	490	7776000	3	8	0	4.9	45	75	D
1/21/2011	2	1.39E-07	0.431	6.84E-06	2.53E-01	4500	82620	7.52E-21	490	7776000	3	8	6.25	4.9	45	43.75	D
1/21/2011	4	6.04E-05	0.431	7.37E-06	2.73E-01	4500	82620	1.86E-23	490	220782	3	8	18.75	4.9	45	0	D
1/21/2011	5	9.75E-03	0.431	9.01E-06	3.33E-01	4500	82620	1.41E-25	490	220782	3	8	31.25	4.9	45	6.25	D
1/21/2011	6	2.94E-01	0.431	9.48E-06	3.51E-01	4500	82620	4.91E-27	490	220782	3	8	37.5	4.9	45	31.25	D
1/21/2011	7	7.08E-04	0.431	1.02E-05	3.77E-01	4500	82620	2.20E-24	490	220782	3	8	25	4.9	45	50	D
1/21/2011	11	3.67E-06	0.431	6.97E-06	2.58E-01	4500	82620	2.90E-22	490	220782	3	8	0	4.9	45	18.75	D
1/21/2011	12	5.25E-06	0.431	7.36E-06	2.72E-01	4500	82620	2.14E-22	490	220782	3	8	6.25	4.9	45	0	D
1/21/2011	13	1.75E-06	0.431	3.32E-06	1.23E-01	4500	82620	2.90E-22	490	220782	3	8	0	4.9	45	87.5	D
1/21/2011	14	8.11E-07	0.431	1.37E-06	5.07E-02	4500	82620	6.34E-21	510	220782	3	9	0	5.1	45	106.25	D
1/21/2011	19	7.45E-07	0.431	1.09E-06	4.03E-02	4500	82620	2.29E-16	600	220782	3	10.4	0	6	45	137.5	D
2/7/2011	9	5.45E-07	0.051	5.31E-06	1.96E-01	4500	33360	8.03E-08	1090	220782	1.3	12.3	0	10.9	45	137.5	B
2/7/2011	11	1.32E-07	0.051	1.39E-06	5.14E-02	4500	33360	2.76E-08	1020	220782	1.3	11.4	0	10.2	45	18.75	B
2/7/2011	13	1.26E-06	0.051	1.32E-05	4.88E-01	4500	33360	2.76E-08	1020	220782	1.3	11.4	0	10.2	45	87.5	B
2/7/2011	14	7.42E-07	0.051	7.53E-06	2.79E-01	4500	33360	3.79E-08	1040	220782	1.3	11.8	0	10.4	45	106.25	B
2/7/2011	17	1.70E-06	0.051	1.54E-05	5.70E-01	4500	33360	2.37E-08	1020	220782	1.3	11.4	6.25	10.2	45	56.25	B
2/8/2011	9	1.51E-07	0.101	1.13E-06	4.18E-02	4500	79740	1.20E-25	450	220782	1.8	12.3	6.25	4.5	45	137.5	E
2/8/2011	10	3.93E-07	0.101	3.10E-06	1.15E-01	4500	79740	1.07E-39	350	220782	1.8	11.4	6.25	3.5	45	75	E
2/8/2011	11	3.10E-07	0.101	2.44E-06	9.03E-02	4500	79740	1.07E-39	350	220782	1.8	11.4	6.25	3.5	45	18.75	E
2/8/2011	12	2.93E-07	0.101	2.31E-06	8.55E-02	4500	79740	1.07E-39	350	220782	1.8	11.4	6.25	3.5	45	0	E
2/15/2012	25	1.04E-06	0.025	6.33E-06	2.34E-01	4500	20460	2.17E-22	490	246952	3.3	8	6.25	4.9	45	56.25	D
2/15/2012	26	1.89E-06	0.025	4.61E-06	1.71E-01	4500	20460	8.70E-23	490	246952	3.3	8	12.5	4.9	45	81.25	D
2/15/2012	27	3.06E-02	0.025	4.27E-06	1.58E-01	4500	20460	4.99E-27	490	246952	3.3	8	37.5	4.9	45	81.25	D
3/6/2012	13	5.37E-07	0.33	1.71E-06	6.33E-02	4500	85200	3.60E-22	490	246952	2.7	8	0	4.9	45	87.5	D
3/6/2012	17	3.10E-07	0.33	9.86E-07	3.65E-02	4500	85200	3.60E-22	490	246952	2.7	8	0	4.9	45	56.25	D
3/6/2012	26	5.23E-05	0.33	1.26E-06	4.66E-02	4500	85200	2.73E-24	490	246952	2.7	8	25	4.9	45	68.75	D
3/8/2013	1	1.51E-01	1.194	1.70E-06	6.29E-02	4500	125880	3.13E-27	490	140844	3	8	37.5	4.9	45	62.5	D
3/8/2013	22	5.78E-06	1.194	5.69E-06	2.11E-01	4500	125880	1.46E-18	550	246952	3	9.5	0	5.5	45	118.75	D
11/12/2013	1	8.76E-04	1.803	2.63E-06	9.73E-02	4500	100800	1.57E-24	490	178909	3.4	8	25	4.9	45	75	D
11/12/2013	21	7.11E-06	1.803	1.82E-06	6.73E-02	4500	100800	4.02E-18	565	140844	3.4	9.75	0	5.65	45	125	D
11/12/2013	23	4.98E-06	1.803	1.34E-06	4.96E-02	4500	100800	7.51E-19	550	178909	3.4	9.5	6.25	5.5	45	118.75	D
2/7/2014	17	7.98E-06	0.508	9.63E-07	3.56E-02	4500	208800	8.58E-24	490	122287	3.6	8	18.75	4.9	45	56.25	D
3/31/2014	18	9.70E-06	0.305	2.04E-06	7.55E-02	4500	23340	2.41E-18	565	178909	7.2	9.75	0	5.65	45	125	D

Table 3. Regression analysis results before imputed values

Coefficients:	Estimate	Std. Error	t value	Pr(>|t|)
(Intercept)	6.438e-01	1.312e+00	0.491	0.649
SFP	-1.706e-01	1.459e-01	-1.169	0.307
Unit 1	-1.214e-02	9.978e-02	-0.122	0.909
Unit 2	-6.911e-02	6.735e-02	-1.026	0.363
Releases	3.742e-06	2.805e-06	1.334	0.253

Table 4. Regression analysis results after imputed values

Coefficients:	Estimate	Std. Error	t value	Pr(>|t|)
(Intercept)	7.137e-01	8.041e-01	0.887	0.404
SFP	-1.950e-01	1.091e-01	-1.787	0.117
Unit 1	-9.542e-03	6.687e-02	-0.143	0.891
Unit 2	-6.948e-02	4.268e-02	-1.628	0.148
Releases	3.566e-06	2.148e-06	1.660	0.141